

# USM3D Analysis of Low Boom Configuration

Melissa B. Carter<sup>1</sup> and Richard L. Campbell<sup>2</sup>  
*NASA Langley Research Center, Hampton VA 23681*

and

Sudheer N. Nayani<sup>3</sup>  
*Analytical Services & Materials, Inc., Hampton, VA 23666*

## Abstract

In the past few years considerable improvement was made in NASA's in house boom prediction capability. As part of this improved capability, the USM3D Navier-Stokes flow solver, when combined with a suitable unstructured grid, went from accurately predicting boom signatures at 1 body length to 10 body lengths. Since that time, the research emphasis has shifted from analysis to the design of supersonic configurations with boom signature mitigation. In order to design an aircraft, the techniques for accurately predicting boom and drag need to be determined. This paper compares CFD results with the wind tunnel experimental results conducted on a Gulfstream reduced boom and drag configuration. Two different wind-tunnel models were designed and tested for drag and boom data. The goal of this study was to assess USM3D capability for predicting both boom and drag characteristics. Overall, USM3D coupled with a grid that was sheared and stretched was able to reasonably predict boom signature. The computational drag polar matched the experimental results for a lift coefficient above 0.1 despite some mismatch in the predicted lift-curve slope.

## Nomenclature

$a_n$	=	GridTool parameter (source propagation proportionality factor which is equivalent to a sphere of influence)
$C_D$	=	drag coefficient
$C_L$	=	lift coefficient
$C_p$	=	pressure coefficient
$H/L$	=	distance below the model normalized by wind-tunnel model length (or body length)
M	=	million
$\Delta p/p$	=	$(p-p_\infty)/p_\infty$
$p$	=	pressure
$p_\infty$	=	free-stream pressure
S-A	=	Spalart-Allmaras turbulence model
SST	=	Shear Stress Transport turbulence model
$x$	=	distance in the stream-wise direction measured from the tip of the nose of the wind-tunnel model, inches.

## I. Introduction

In 2007, the state of art gridding technique for boom prediction for NASA Langley Research Center's USM3D/TetrUSS CFD package was from a sourcing method produced by Wyle Labs in 2004 under NASA contract NAS1-98100. This grid sourcing method involved sources coming from the body at the expected Mach angle and continued into the far field one body length below the aircraft. An additional set of line sources were used to form a cylinder around the aircraft with a radius of one body length. These sources and their locations, had to be

---

<sup>1</sup> Aerospace Engineer, Configuration Aerodynamics Branch, MS 499, AIAA Senior Member.

<sup>2</sup> Senior Research Engineer, Configuration Aerodynamics Branch, MS 499, AIAA Associate Fellow.

<sup>3</sup> Senior Scientist, CFD Group, 107 Research Drive, AIAA Senior Member.

manually calculated and inserted. Since the fine grid sources extended to one body length, the computational prediction matched well there. However at 2.5 body lengths the predicted signature loses crispness and did not predict the initial shock or the recovery. In 2008, several breakthroughs in grid production, manipulation, and adaptation shifted the state-of-the-art boom prediction capability up to 10 body lengths below the aircraft.<sup>1,2</sup> The new process involved the inclusion of a volume source directly underneath the aircraft<sup>3</sup> and the use of a postprocessor, SSGRID<sup>3</sup>, to shear and stretch the grid in the direction of the shock (figure 1).

As NASA's Fundamental Aeronautics Program Supersonics Project has progressed, the goal has evolved to be able to design and analyze a configuration for low-boom and low-drag performance. In order to design an aircraft, the techniques for accurately predicting boom and drag individually need to be determined. The CFD codes need to be assessed to see if the flow physics for both boom and performance can be simultaneously modeled. In addition, the grid resolution and grid adaptation techniques for predicting boom and drag are different. It would be advantageous if the differing parts of the gridding requirements were minimized between the drag and boom simulations.

As a first step in this direction, numerical simulations were conducted to represent recent wind-tunnel experience on a low drag, low boom configuration. These simulations were conducted using configurations provided by the Gulfstream Aerospace Corporation. Two different experimental wind-tunnel models, one for drag and one for boom, were created for testing. Several differences in the geometries exist and include: type and location of the sting for testing, the aft fuselage closure, the size of the wind-tunnel model and the testing conditions that the experimental data was obtained. Due to these differences, the computational studies were conducted on the appropriate Computer-aided Design (CAD) representations of these wind-tunnel models. Grid convergence and best practice studies were conducted to best replicate the experimental test data. This paper describes the effects of a laminar boundary layer as well as turbulence modeling and gridding techniques implemented for the boom and drag wind-tunnel models, respectively.

## II. Computational Method

This computational fluid dynamics (CFD) study used the NASA Tetrahedral Unstructured Software System (TetrUSS<sup>6</sup>) for all the computations. This CFD suite, created and maintained at NASA Langley Research Center, includes an unstructured grid generation program called VGRID, a postprocessor named POSTGRID, and the flow solver USM3D.

VGRID is an interactive or batch tetrahedral unstructured grid generation program. The grids produced by VGRID are suitable for computing Euler or Navier-Stokes flow solutions. The grid spacing is related to the strength of user-defined sources placed in the domain. The methodology is based on the Advancing-Front method (AFM)<sup>7</sup> and the Advancing-Layers method (ALM).<sup>8</sup> Both techniques are based on marching processes in which tetrahedral cells are grown on an initial triangular boundary mesh and gradually form in the field around the geometry. Once the advancing front process is completed in VGRID, an additional post-processing step is required using POSTGRID to close any open pockets and improve grid quality. For the boom geometry, the NASA Langley code SSGRID was used to stretch and shear the grid.<sup>3</sup>

The unstructured grids are sheared and stretched in order to reduce dissipation and better capture the near-field sonic boom signature below an aircraft. In general, the grid is sheared to bring it into closer alignment with the free-stream Mach angle, so that pressure changes across features such as shocks are better captured in a direction normal to cell faces. The grid stretching contributes to this alignment process by giving the cells a longer face in the direction of the Mach angle. In addition, the stretching appears to further reduce the dissipation by reducing the number of cells between the aircraft surface and the signature location. The code defines a region close to the aircraft surface where the grid is not stretched. In addition to preserving the surface geometry, this is required to avoid distorting the boundary layer grid for viscous cases.

The USM3D code<sup>9</sup> is a cell-centered, finite-volume Navier-Stokes flow solver that uses Roe flux-difference splitting<sup>10</sup> to compute inviscid flux quantities across the faces of the tetrahedral cells. Several options for turbulent closure are available: the one-equation Spalart-Allmaras (S-A) turbulence model<sup>11</sup> (with and without a wall function), and several two-equation turbulence models, including Menter's Shear Stress Transport (SST) turbulence model.<sup>12</sup> The parallel version of the flow solver was run at the NAS Supercomputing facility on large Linux clusters at NASA Ames Research Center. Grid sizes up to 27 million cells were run on the Columbia supercomputer and a typical run took about 650 CPU hours when 64 processors were used. Grid sizes of 31 million cells and above were run on the Pleiades supercomputer and a typical run took about 900 CPU hours when 96 Westmere processors were used. Most of the results presented in this paper are at Mach 1.6. Under these supersonic conditions USM3D will, most of the time, require a limiter (minmod limiter in this case) for proper convergence.

The choice of turbulence model used proved to be very important to the boom case, as discussed below. Consequently, the S-A turbulence model, the SST turbulence model and running the code laminar were all used on the boom configuration. For the drag geometry, both the SST and S-A turbulence models were assessed, however all of the data presented in this paper are results from the S-A model, also discussed below. All of the grids were generated to be fully viscous grids (no wall-modeling was used) with a  $y^+$  value of less than or equal to 0.5. The average convergence of the residual for all the runs were between 3.5 and 4 orders of magnitude. The force coefficients were also monitored, and the CFD run was not terminated until the force coefficients converged (the change in results were less than 0.5%).

### **III. Experimental Testing Information**

#### **A. Boom Testing**

The boom testing<sup>4</sup> was performed at NASA Langley Research Center in Hampton, Virginia. The test was conducted in the 4-foot Supersonic Unitary Plan Wind Tunnel (UPWT). There are two sections at UPWT which together can obtain speeds from Mach 1.5 to Mach 4.6 and Reynolds numbers per foot up to  $11 \times 10^6$ . The system operates as a closed circuit with a test section size of 4' by 4' by 7' long.<sup>13</sup>

A wind-tunnel model of 13.2 inches in length was used during this test. Since the objective of this test was to obtain the boom signature at specified H/L locations below the wind-tunnel model, the blade sting was integrated into the upper surface so that its effect on the pressure signature would be shielded by the wind-tunnel model (figure 2). The experimental data presented below was obtained at a Mach number of 1.6, angles of attack from 0.24 to 0.27 degrees, and at unit Reynolds number of 3.5 million per foot which corresponded to a Reynolds number, based on mean aerodynamic chord, of 0.613 million, or a Reynolds number, based on wind-tunnel model length, of 3.85 million.

All of the runs, except for a repeat run of the H/L equal to 1.7, were conducted with free transition. The repeat run at an H/L of 1.7 had the transition fixed as shown in figure 3. At these Reynolds numbers, laminar and transitional flow could be expected. Consequently, the free transition results proved to be challenging to replicate computationally, as discussed below.

#### **B. Drag Testing**

Drag testing<sup>5</sup> was conducted in the 8x6 Supersonic Wind Tunnel (SWT) at NASA Glenn Research Center in Cleveland, Ohio. The test section is 8' by 6' by 23.5' long. A flexible wall nozzle upstream from the test section is used to accelerate the free-stream airflow. The system was operated in a closed-loop cycle which allows the tunnel to obtain speeds as high as Mach 2.0 and Reynolds number per foot up to  $4.8 \times 10^6$ .<sup>14</sup> Experimental data presented was obtained at a Mach number of 1.55, at 15 angles of attack varying from -5.8 to 6.5 degrees, and at a unit Reynolds number of 4.82 million per foot which corresponded to a Reynolds number, based on mean aerodynamic chord, of 3.36 million, or a Reynolds number, based on wind-tunnel model length, of 21.12 million.

The larger test section of SWT enabled use of a wind-tunnel model of 52.8 inches in length which enabled greater model fidelity than the 13.2 inches in length model used in the UPWT test. The objective of the test was to determine configuration forces and moments. Therefore, the configuration was designed to accommodate a standard straight sting protruding from the aft of the aircraft (figure 4).

### **IV. Gridding Procedure and Results**

#### **A. Boom Configuration**

The wind-tunnel boom geometry was provided by Gulfstream. Grid sourcing was done using AutoSrc<sup>15</sup> code using an overall sourcing factor of one. Line sources were used on the geometry surface and a cylindrical source was placed underneath the aircraft for capturing the near-field boom pressure signature. The nose had a sharp point, and the vertical tail, wing, and aft fuselage annulus around the sting had sharp trailing edges. Sourcing these patches proved to be challenging as they were giving flat (zero height) cells, which would cause during volume grid generation. This problem was alleviated by stretching the sources at the sharp corners (~20 aspect ratio).

Once the volume grid had been generated, the grid below the configuration was stretched using the SSGRID code in the Mach angle direction. The resulting grid has stretched cells to provide an aspect ratio of approximately 40, both at the top and bottom of the cylindrical volume source. A utility code was used to remove the negative volume cells during the post-processing step. A grid sensitivity study was carried out by generating 3 grids (20, 27

and 34 million cells) and it was found that force coefficients did not change significantly; there was less than 1% difference in force results between the 27 and 34 million cell grids.

A sample solution showing the pressure distribution below the geometry is shown in figure 5. The case, ran as fully laminar at Mach 1.6 shows the alignment of the grid and the stretching with flow solution. The three lines below the geometry show the H/L locations of 0.49, 1.2 and 1.7 where experimental data was obtained. The figure shows that the effects of the change in geometry of the nose spike can be clearly seen in the solution along with the shock-expansion effects from the main components of the aircraft.

Computational assessments were performed with two turbulence models as well as with laminar flow. The S-A turbulence model, the most commonly used model with in the code was assessed. Since the S-A turbulence model has been shown by colleagues to not do as well with sonic boom when the initial cell height of the grid is very small, the SST turbulence model was also assessed.

The results from this part of the study can be seen in figures 6, 7, and 8. The experimental data was obtained at Mach 1.6 and H/L of 0.49, 1.2 and 1.7, where H is the distance below the geometry and L is the body length of the model. The experimental angle of attack for all the data varied slightly around 0.256 degrees (0.24-0.27 degrees). Figure 6 compares the experimental results with CFD at a H/L of 0.49, and angle of attack of 0.256 degrees. Note: experimental data was not available for X/L values less than 1 at this H/L. As shown in figure 6, the S-A results failed to capture the initial compression or the extent of the expansion. SST proved to do better at predicting the main compression and recovery then the S-A turbulence model, but still did not match the experimental data. Although the laminar case does not predict the full strength of the main compression, it does excellent in matching the rest of the experimental data. Figures 7 and 8 compare the experimental data with CFD for H/L of 1.2 and 1.7, respectively, at an angle of attack of 0.256 degrees. Both cases show that the CFD study results conducted with fully laminar flow does good at matching the experimental data through the nose spike region, forward body and the main expansion and recovery, but underestimates the strength of the main compression. Due to the test conditions and the free transition, these results are not surprising. Figure 8b compares the results with both sets of experimental data at H/L of 1.7. The H/L of 1.7 case was the only case where data was obtained with both free and fixed transition. Overall, when the transition is fixed, the SST turbulence model did excellent in matching the experimental results.

## **B. Drag Configuration**

The 52.8 inch long wind-tunnel model tested at NASA Glenn was the basis for this part of the CFD simulation. This geometry was different from the boom geometry: trailing edges were thicker and the wind-tunnel model had the traditional sting in the back as opposed to the boom wind-tunnel model which had the blade sting in the middle of the fuselage. Consequently, the aft fuselage closure was significantly different between the two geometries. The sourcing strategy was the same as that of the boom model and the AutoSrc<sup>15</sup> code was used for sourcing without the cylindrical source underneath the configuration. Generating finer grids proved to be challenging as the patches near the wing tip were quite sensitive to smaller source spacing. The issue was circumvented by removing the source stretching in this area and also making the 'a<sub>n</sub>' parameter greater than 1 in GRIDTOOL (a pre-processor for VGRID). A grid sensitivity study was conducted by generating 4 grids (16, 27, 31 and 42 million cells) and it was determined that the force coefficients remained converged (less then 0.5% change in value). Due to the size of the 42 million cell grid, only one condition was computed and compared to the 31 million cell grid to confirm convergence (not shown). The 31 million cell grid was selected as the final grid and solutions were obtained for all 15 angles of attack. Flow solutions were obtained both with and without the limiter for all angles of attack. Two turbulence models, the two equation SST and the one equation fully-viscous (as opposed to wall-function) Spalart-Allmaras (S-A) turbulence model, were used in generating the numerical results. For the scope of this assessment, the S-A turbulence model gave results closer to the experimental data, and thus all of the force data presented in this paper is with the S-A model.

The results can be seen in figures 9 and 10. Figures 9 shows that although the grid solutions converged to similar values, the CFD did not match experimental angle of attack trend for the lift coefficient. The computational results matched the experimental drag polar fairly well for a C<sub>L</sub> greater then 0.10, as shown in figure 10. Although most of the cases show reasonable agreement between the CFD and experimental results, runs conducted without the limiter matched the experimental data better then the runs with the limiter at the lower C<sub>L</sub> levels. This can be seen clearly in the inset graph in figure 10. These results were somewhat expected; our past experience has shown that using the midmod limiter within USM3D affects drag data.

## V. Future Work

One aspect of the experimental testing that is not addressed in this study is off-track boom signature predictions; i.e., ones obtained not directly below the wind-tunnel model. Figures 11 and 12 compare results from boom grid with experimental data for off-track boom signature predictions. Figure 11 shows that USM3D/SSGRID does reasonably predicting the boom at 26-degrees off track although it is underestimating the signature of the nose spike, and the strength of the main compression and expansion. Figure 12 shows that when looking at the 38.5-degrees off track results, USM3D/SSGRID has completely lost the signature affects due to the nose spike. This is not surprising, since, as mentioned in the Computational Methods section, the stretching approach used does not include a radial component. The results presented are due to a lack of specialized sourcing and stretching that can be done for boom signatures directly below the wind-tunnel model. Future work includes testing and if possible, adding this capability to VGRID.

Another aspect of future work is to examine the criteria for running boom cases with the limiter off. Successful runs have been made on other configurations with the limiter turned off and the grid highly sheared and stretched.

Finally, a future test where both drag and boom data is obtained, using the same configuration and experiencing the same flow conditions is planned and the results should assist with future studies.

## VI. Conclusion

USM3D can predict boom, when paired with SSGRID, and drag characteristics. The experimental boom data obtained without fixing the transition proved to be challenging to match since the flow may have been laminar and transitional on the wind-tunnel model due to the low Reynolds number. The fully laminar case best matched the experimental results. However, for the one case with a fixed transition, the results from the SST turbulence model overall matched the experimental data.

Since the overall goal is to attempt to predict boom and drag from the same computational model, this study has identified two difficulties that must be overcome. Predicting boom and drag required two different turbulence models in order to best match the experimental data. Additionally, in order to run the highly stretched and sheared grid cells necessary to obtain the boom signature, the midmod limiter had to be used. The drag study showed that using the midmod limiter does negatively affect the force calculations.

## Acknowledgments

The work done was sponsored by NASA Fundamental Aeronautics Program Supersonics Project. The majority of the computational runs and grid generations were conducted by of Analytical Services & Materials, Inc. under contract NNL09AM01T.

## References

- <sup>1</sup> Pirzadeh S., "Advanced Unstructured Grid Generation for Challenging Aerodynamics Applications." AIAA-2008-7178, August 2008.
- <sup>2</sup> Carter, M. and Deere, K., "Grid Sourcing and Adaptation Study Using Unstructured Grids for Supersonic Boom Prediction." AIAA Paper 2008-6595, 2008.
- <sup>3</sup> Campbell, R. C.; Carter, M. B.; Deere, K.A.; and Waithe, K. A., "Efficient Unstructured Grid Adaptation Methods for Sonic Boom Prediction." AIAA-2008-7327, August 2008.
- <sup>4</sup> Wayman, T., "Near Field Acoustic Test on a Low Boom Configuration in Langley's 4 x 4 Wind Tunnel." AIAA-2011-3331, June 2011.
- <sup>5</sup> Wayman, T., "Force and Moment Test on a Low Boom Configuration in Glenn's 8 x 6 Wind Tunnel." AIAA-2011-3332, June 2011.
- <sup>6</sup> Frink, N. T.; Pirzadeh, S.Z.; Parikh, P.C.; Pandya, M.J.; and Bhat, M.K., "The NASA Tetrahedral Unstructured Software System", The Aeronautical Journal, Vol. 104, No. 1040, October 2000, pp. 491-499.
- <sup>7</sup> Lohner R and Parikh P., "Three-Dimensional Grid Generation by the Advancing Front Method." Int.J.Num.Meth. Fluids 8, pp 1135-1149 (1988).
- <sup>8</sup> Pirzadeh S., "Three-dimensional unstructured viscous grids by the advancing layers method." AIAA Journal, Vol. 34, No. 1, January 1996, pp. 43-49.
- <sup>9</sup> Frink, N. T., "Three-Dimensional Upwind Scheme for Solving the Euler Equations on Unstructured Tetrahedral Grids", Ph. D. Dissertation, Virginia Polytechnic Institute and State University, September 1991.

<sup>10</sup> Roe, P., "Characteristic Based Schemes for the Euler Equations." Annual Review of Fluid Mechanics, Vol. 18, 1986, pp. 337-365.

<sup>11</sup> Spalart, P.; and Allmaras, S.A., "One-equation turbulence model for aerodynamic flows." AIAA 92-0439, January 1992.

<sup>12</sup> Menter, F.R., "Improved Two-Equation k- $\omega$  Turbulence Models for Aerodynamic Flows." NASA TM-103975, October 1992.

<sup>13</sup> Ground Facilities and Testing Directorate at NASA Langley. NASA NP-2010-02-243-LaRC

<sup>14</sup> Soeder, R. H., "NASA Lewis 8- By 6-Foot Supersonic Wind Tunnel User Manual." NASA TM-105771, February 1993.

<sup>15</sup> Li, Wu; Campbell, Richard; Geiselhart, Karl; Shields, Elwood; Nayani, Sudheer; Shenoy, Rajiv, "Integration of Engine, Plume, and CFD Analyses in Conceptual Design of Low-Boom Supersonic Aircraft." AIAA 2009-1171, January 2009.

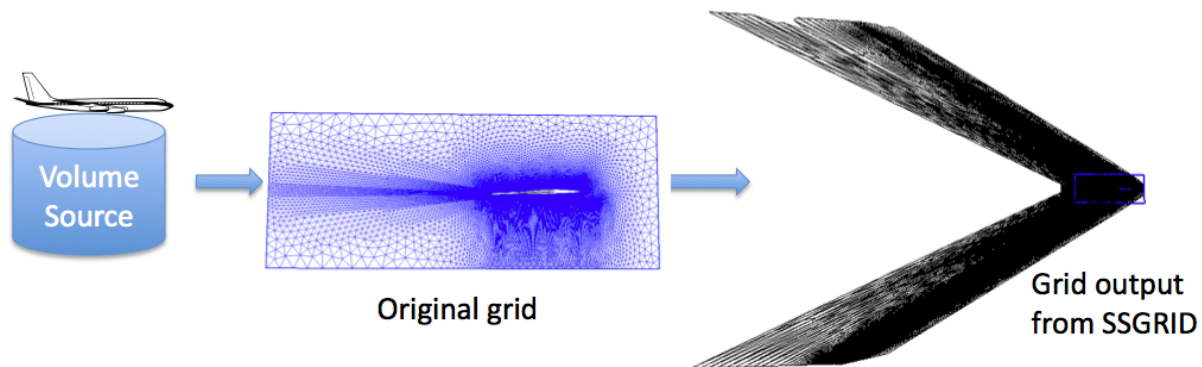


**Figure 1. Gridding method combined with SSGRID to produce stretched and sheared grid.**

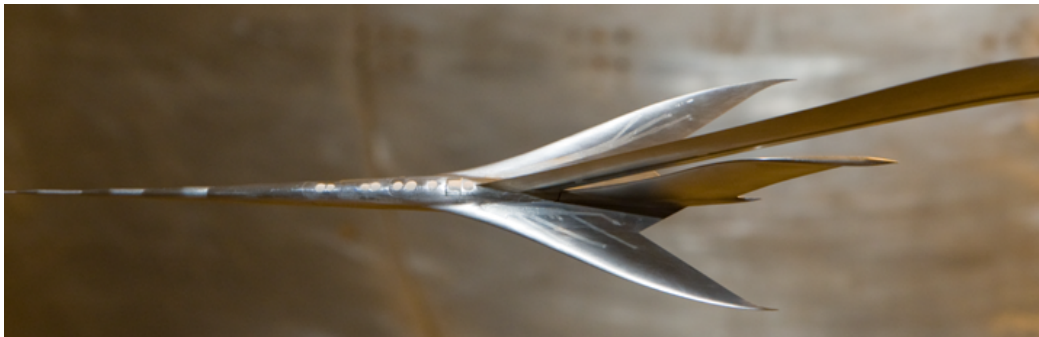


**Figure 2. Boom experimental model.**

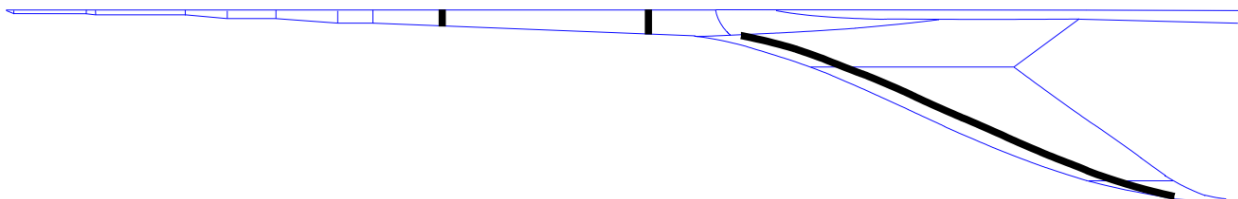


**Figure 3. Grit locations used for 1.7 H/L experimental boom data run.**

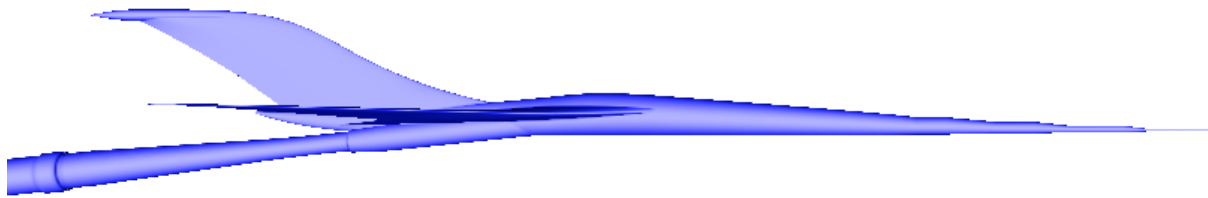
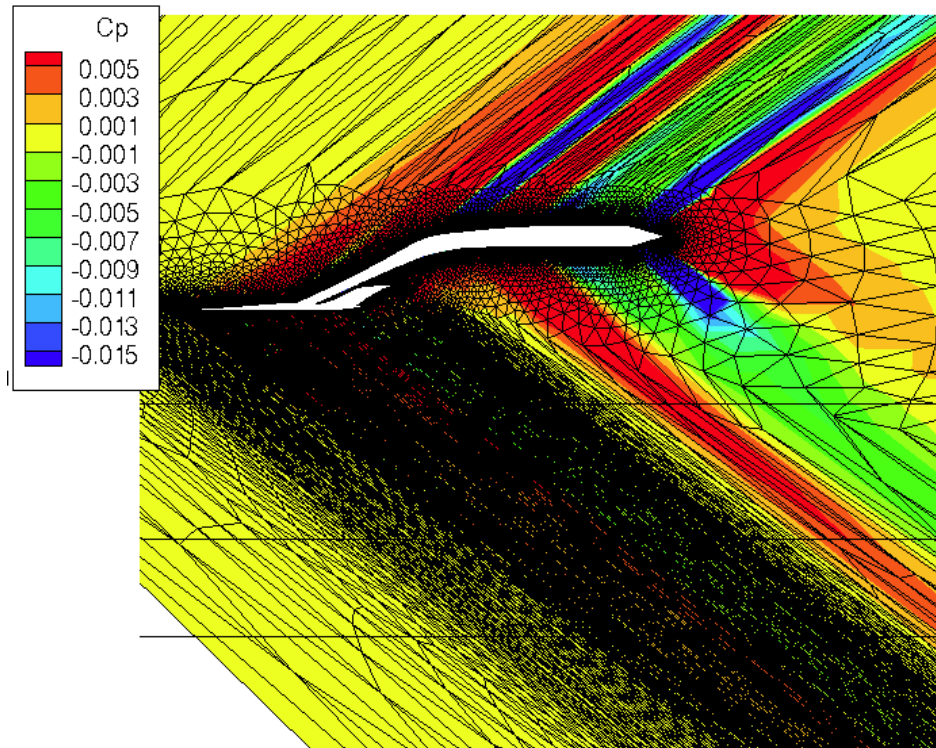
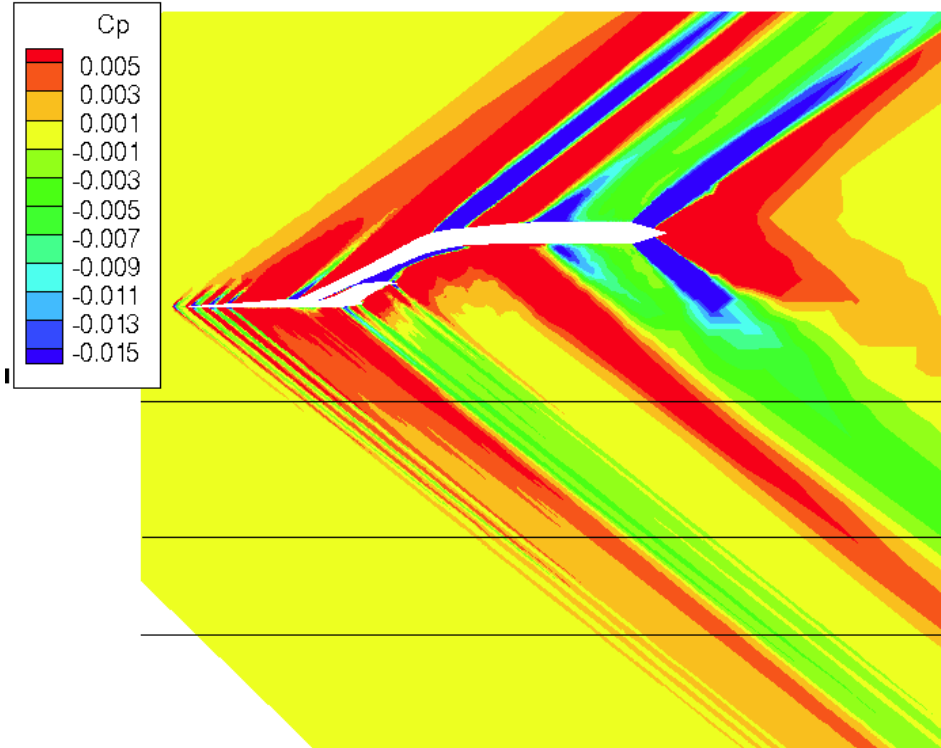


**Figure 4. Computational model of drag experimental model.**



**a) Laminar flow Cp results and corresponding grid at Mach =1.6, alpha =0.256 degrees.**



b) Laminar flow  $C_p$  results at Mach =1.6,  $\alpha$  =0.256 degrees.

Figure 5.  $C_p$  results from Laminar case with H/L locations of 0.49, 1.2 and 1.7 shown.

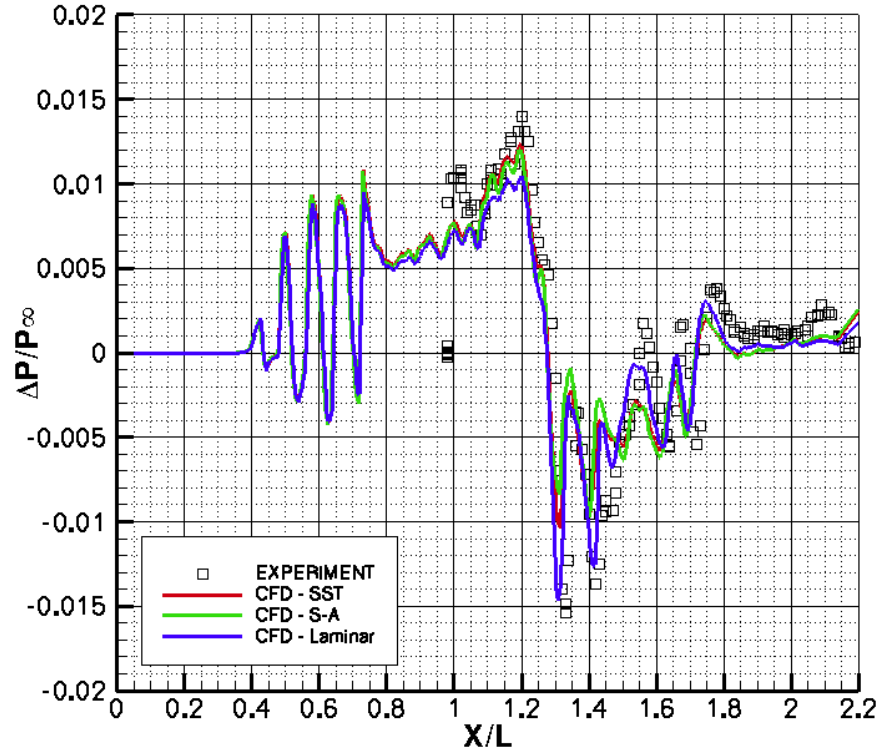


Figure 6. Boom signature comparison of 34M boom grid at H/L =0.49, Mach =1.6,  $\alpha$  =0.256 degrees.



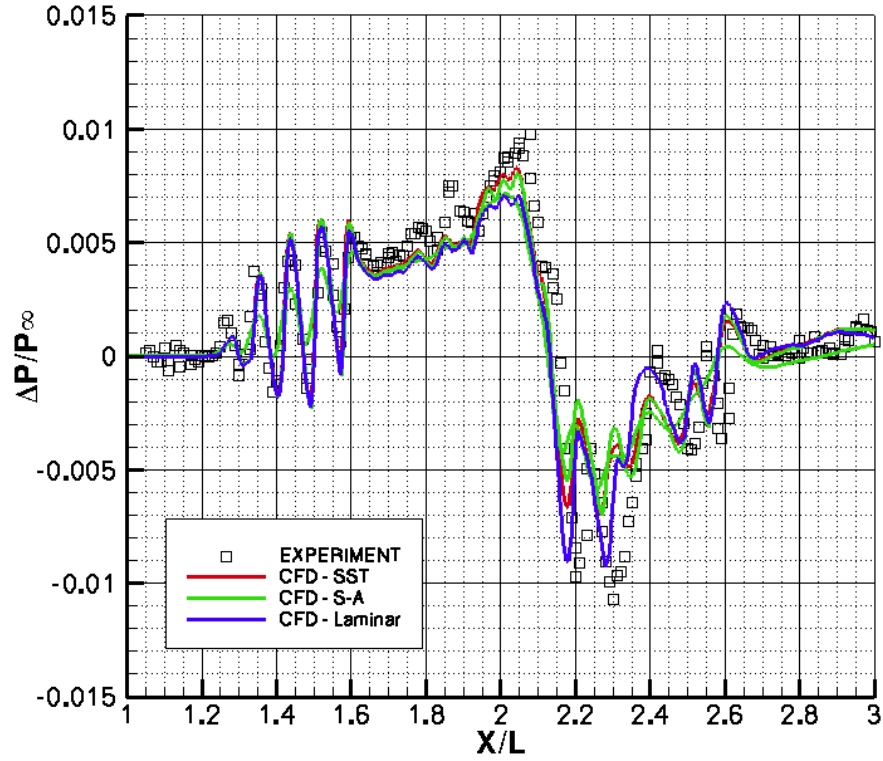
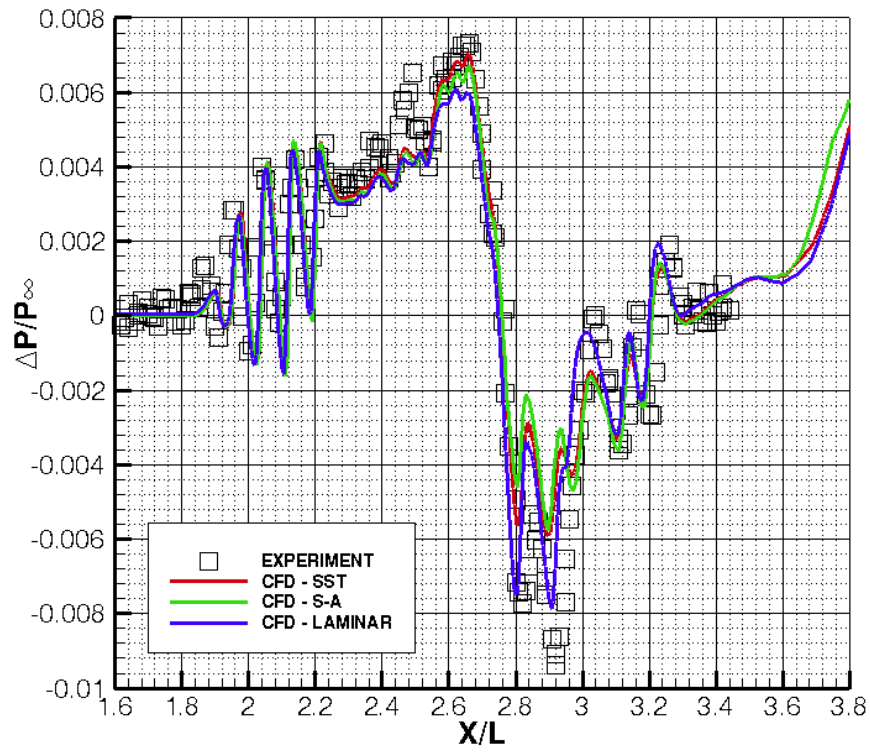


Figure 7. Boom signature comparison of 34M boom grid at  $H/L = 1.2$ ,  $Mach = 1.6$ ,  $\alpha = 0.256$  degrees.



a) Free transition

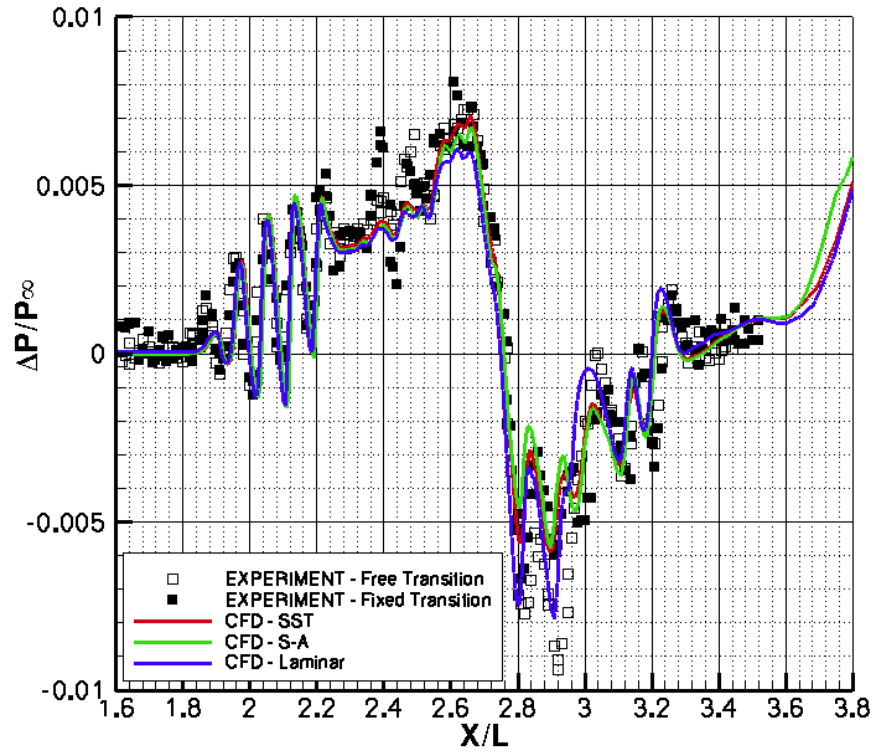


Figure 8. Boom signature comparison of 34M boom grid at  $H/L = 1.7$ ,  $Mach = 1.6$ ,  $\alpha = 0.256$  degrees.

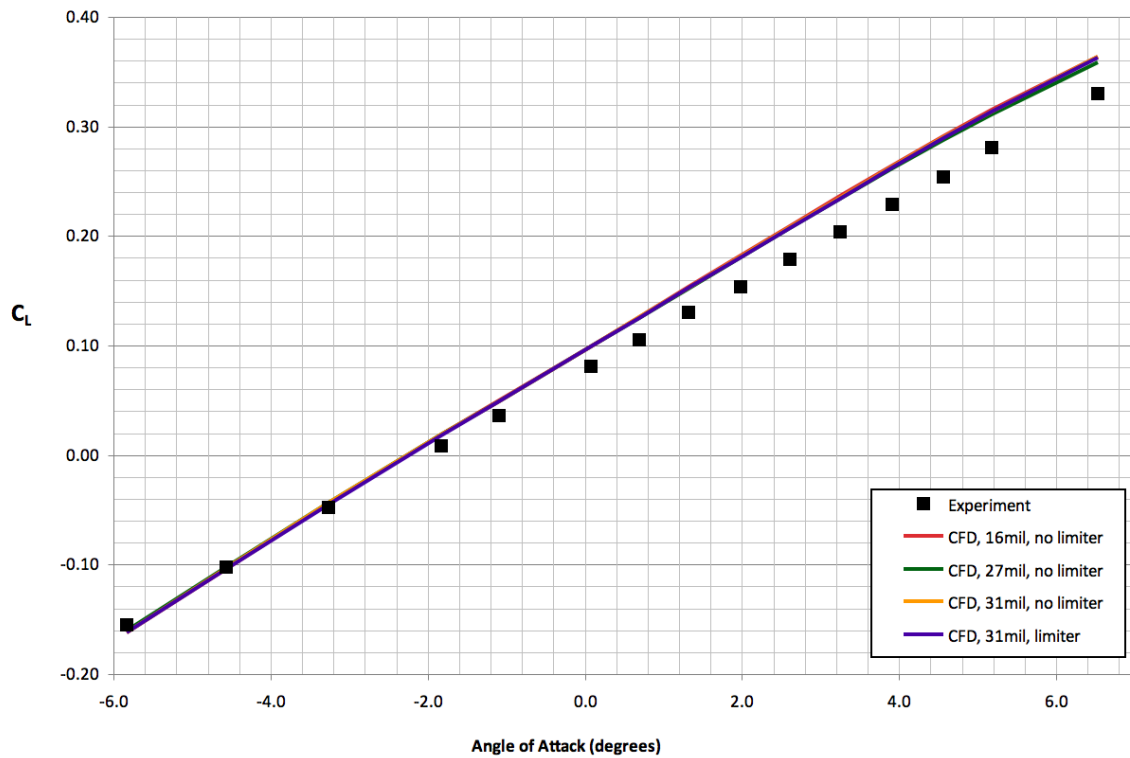


Figure 9. Lift coefficient vs.  $\alpha$  results from grid study conducted on drag model,  $Mach = 1.55$ .

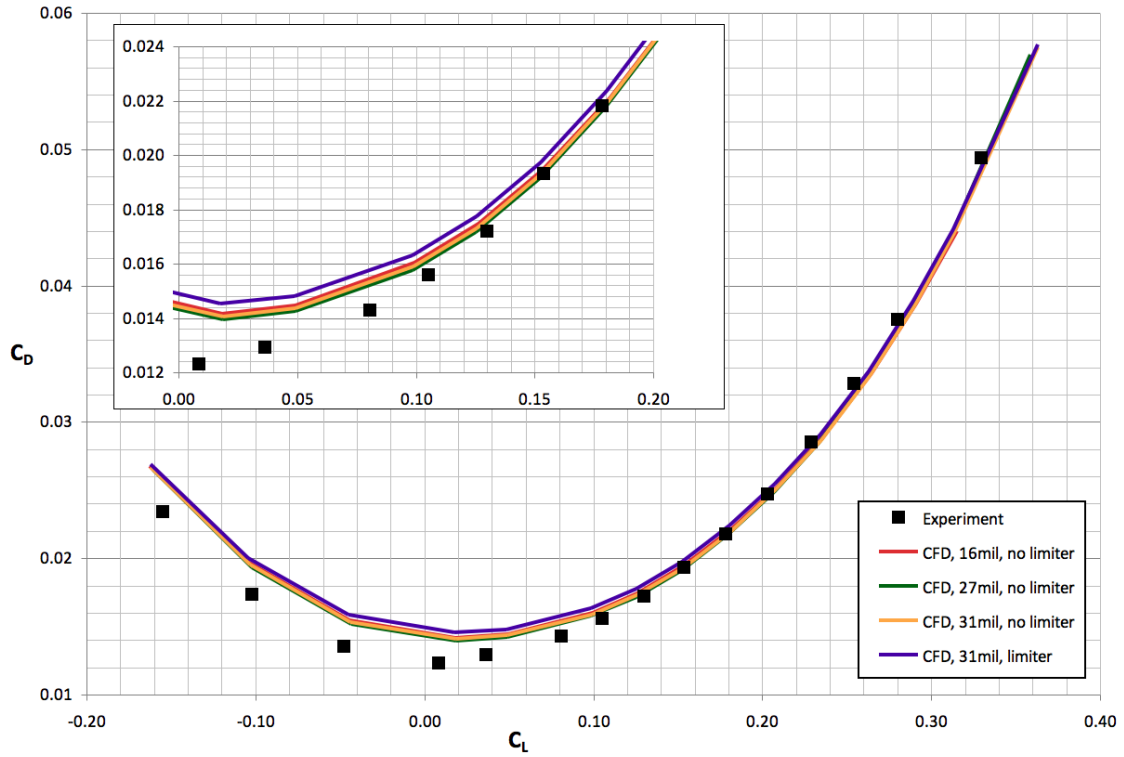


Figure 10. Drag coefficient vs. lift coefficient results from grid study conducted on drag model including runs with and without limiter, Mach =1.55

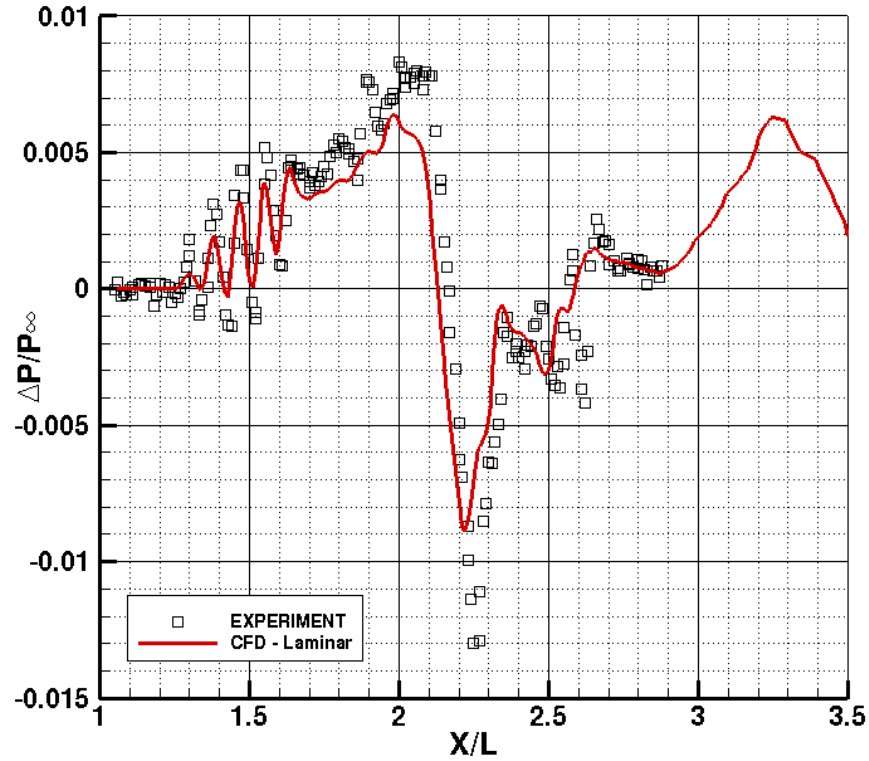


Figure 11. 26-Degree off-track boom signature comparison of 34M boom grid at  $H/L=1.201$ , Mach =1.6,  $\alpha=0.256$  degrees.

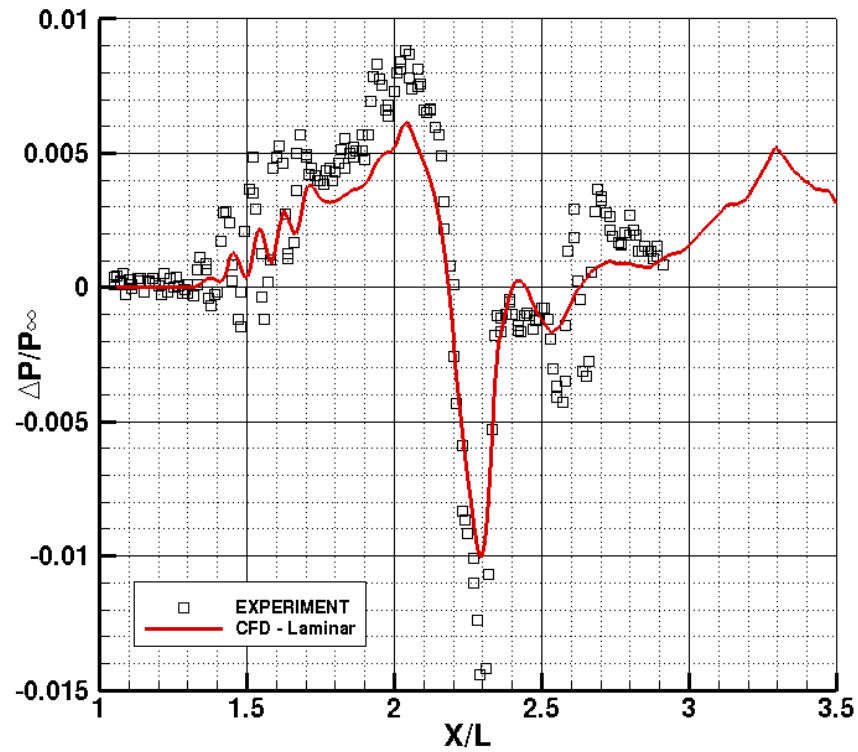


Figure 12. 38.5-Degree off-track boom signature comparison of 34M boom grid at  $H/L = 1.23$ ,  $Mach = 1.6$ ,  $\alpha = 0.256$  degrees.